

Nanografting De Novo Proteins onto Gold Surfaces

Ying Hu,[†] Aditi Das,[†] Michael H. Hecht,^{*,†,‡,§} and Giacinto Scoles^{*,†,‡,§}

Chemistry Department, Princeton Institute for the Science and Technology of Materials (PRISM), Princeton University, Princeton, New Jersey 08544, and International School for Advanced Studies and Elettra Synchrotron Laboratories, Trieste, Italy

Received December 19, 2004. In Final Form: July 12, 2005

The immobilization of novel proteins onto addressable locations on a flat surface has potential applications in a range of biotechnologies. Here we describe the nanopatterning of a de novo protein onto a gold surface. Patterning was achieved using a technique called nanografting, in which the tip of an atomic force microscope is used to disrupt a preexisting monolayer of alkanethiol molecules on a gold surface, thereby facilitating exchange with alternative thiol-linked molecules from the surrounding solution. The protein used for these studies was chosen from a designed combinatorial library of de novo sequences expressed in *E. coli* and was engineered to have a glycine-glycine-cysteine tag at its C-terminus, thereby enabling attachment to the gold surface through a single cysteine thiol. The average height of the grafted protein patterns was found to be somewhat higher than expected from the known NMR structure of the protein. Compression of the nanografted patches by an external force (below 10 nN) was reversible but showed some hysteresis. Interestingly, both the energy required to deform the immobilized protein patterns and the energy defined by the hysteresis loop were found to be of the same order as the energy required to unfold the monomeric protein in solution. These studies demonstrate the possibility of preparing nanometer scale protein arrays, lowering significantly the volume requirements of the protein samples necessary to fabricate protein-based biosensor arrays and thereby providing a base for increasing their sensitivity.

Introduction

Substantial effort has been directed toward the construction of biosensors on the nanometer scale.^{1,2} Biosensors are analytical devices that (i) use biological molecules to incorporate molecular recognition and/or catalyze reactions at a surface and (ii) use a physical transducer to translate this recognition and/or catalysis into optical, electrical or magnetic signals.² Although considerable research in this field has focused on “DNA chips”, recent progress in proteomics highlights the need for protein microarrays.³ The use of microarrays to probe protein activity has several advantages: Each protein can be addressed individually; multiple identifications can be carried out in a single round under well defined conditions; and identification procedures are relatively fast.⁴ To take full advantage of this technique, it is important to control the spatial arrangement of the proteins. To achieve such control, several techniques are available: These include microcontact printing, dip-pen nanolithography, ink-jet printing, and photolithography.⁵

Moving from the microscale to the nanoscale offers several advantages: The quantities of sample required are reduced, each pattern may be more homogeneous because of its smaller size, and specific interactions between proteins can be observed at higher resolution. The knowledge obtained from nanoscale studies can be used to design nanoscale detectors for future technological applications.

Nanoscale biosensors that use proteins are particularly attractive because molecular recognition sites with high affinity and exquisite selectivity for specified target molecules can be found in natural proteins or can be engineered into artificial proteins.²

Early attempts to construct protein-based biosensors relied on natural proteins.⁶ However, because natural proteins have evolved to perform particular functions in specific biological environments, they may not be optimal for certain technological applications. In contrast, proteins designed de novo can potentially be “tailor-made” for specified applications. Consequently, for the current studies, we focused on a protein isolated from a large combinatorial library of de novo amino acid sequences.

Proteins can be immobilized on a surface either by physical adsorption or through specific chemical linkers. When proteins are physically adsorbed onto a surface, their orientations relative to the surface can be difficult to control. Moreover, randomly oriented physical adsorption can disturb the tertiary structure of the protein, and hence its structure-dependent functionality. To design effective biosensors, it is crucial to control the coupling of the de novo protein to the detecting surface. Therefore, for the current studies, we engineered a unique chemical linkage (the thiol of a C-terminal cysteine) into our protein, thereby providing a unique site for immobilization.

The AFM-based nanografting technique introduced by Liu in 1997 has distinct advantages in that it enables the coupling of a protein to a surface without disturbing its tertiary structure.⁷ The basic idea of nanografting is to use an AFM tip to disturb the original molecules (e.g., thiols on gold) from a specified area of a monolayer, thereby enabling different thiol molecules from a contacting

* To whom correspondence should be addressed. E-mail: gscoles@princeton.edu (G.S.); hecht@princeton.edu (M.H.H.).

[†] Chemistry Department.

[‡] Princeton Institute for the Science and Technology of Materials (PRISM).

[§] International School for Advanced Studies and Elettra Synchrotron Laboratories.

(1) Turner, A. P. F. *Science* **2000**, *290*, 1315–1317.

(2) Gilardi, G.; Fantuzzi, A. *Trends Biotechnol.* **2001**, *19*, 468–476.

(3) MacBeath, G.; Schreiber, S. L. *Science* **2000**, *289*, 1760–1763.

(4) Phizicky, E.; Bastiaens, P. I.; Zhu, H.; Snyder, M.; Fields, S. *Nature* **2003**, *422*, 208–215.

(5) Chrisey, D. B. *Science* **2000**, *289*, 879–881.

(6) (a) Hellinga, H. W.; Marvin, J. S. *Trends Biotechnol.* **1998**, *16*, 183–189. (b) Boussaad, S.; Tao, N. J. *J. Am. Chem. Soc.* **1999**, *121*, 4510–4515.

(7) (a) Xu, S.; Liu, G. Y. *Langmuir* **1997**, *12*, 127–129. (b) Liu, G. Y.; Xu, S.; Qian, Y. *Acc. Chem. Res.* **2000**, *33*, 457–466.

solution to self-assemble by diffusion or exchange onto the exposed gold sites. The surface can be imaged at a low force and then patterned with different molecules at a higher force. Because imaging and patterning are accomplished using the same tip under the same conditions, tip-induced and environmentally variable effects on reproducibility can be minimized. Moreover, nanografting can be used not only to pattern a surface at the nanometer scale, but also to pattern and visualize several different monolayer patches at several different addressable locations.

Compared to the widely used patterning method of microcontact printing, nanografting, being a serial procedure, is a slower tool for nanofabrication. However, once the initial nanografted surfaces have been constructed, these patterns have the possibility to be used for pattern transfer in a manner analogous to the way that masks made by e-beam lithography are used for pattern transfer in microcontact printing.⁸ However, nanografting as a lithographic technique has much higher resolution than microcontact printing. Moreover, since the nanografting procedure is carried out in aqueous solutions, nanografted proteins are more likely to retain their bioactivity.

Another significant advantage of nanografting is that the nanografted patches are normally better ordered than the surrounding monolayer.⁷ This leads to the possibility of controlling the orientation and the packing of proteins. Having a well-organized protein patch has several advantages: First, in contrast to individual protein molecules, which would be easily bent or influenced by the AFM tip, dense patches of protein are likely to be more stable and therefore more resistant to the force exerted by the AFM tip. This enables one to study the height of these patches and their response to external forces. Second, although measuring the binding affinity or electron-transfer properties of a single protein is difficult, these measurements become easier with a protein patch.⁹ Finally, given the notorious reluctance of membrane proteins to crystallize, studies of nanografted protein patches, which resemble proteins in a membrane (at least half a membrane), may provide insights that pave the way toward achieving two-dimensional crystallization of membrane proteins.

The packing of proteins into patches also presents several challenges: For example, tight packing may interfere with the natural recognition and catalytic functions of a protein. By learning to control and measure packing density, we hope, eventually, to turn this drawback into an opportunity to study how protein–protein interactions influence both protein–ligand recognition and enzymatic activity.

Here we report the nanografting and characterization of a de novo 4-helix bundle protein onto the (111) surface of gold. The particular protein used here was engineered to contain a Gly-Gly-Cys linker at its C-terminus. The terminal cysteine provides a thiol bridge for attachment to the gold surface. This protein, which we call S-824-C, was derived from a previously reported protein, S-824. S-824 and S-824-C have the same amino acid sequence, except that the former lacks the engineered C-terminal tripeptide linker. The “parental” S-824 protein was chosen from a library of 102-residue sequences designed to fold

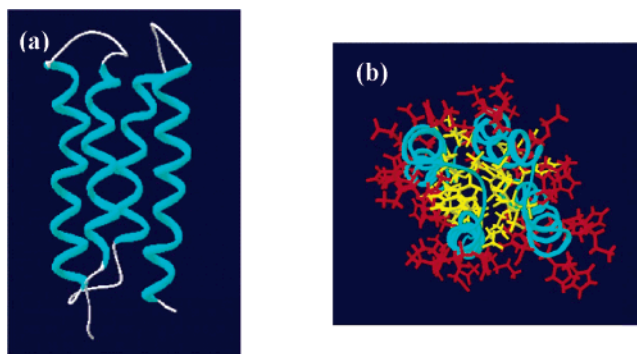


Figure 1. (a) Ribbon diagram of the solution structure of the four helix bundle protein S-824.¹⁰ (b) Head-on view of the structure shows that nonpolar side chains (yellow) form the hydrophobic core while polar side chains (red) are exposed to the solvent, as specified by the design.

into 4-helix bundles.^{10,11a} This library was designed using the “binary code” strategy, in which each position in an amino acid sequence is designed to be either polar or nonpolar, but the exact identity of each polar and nonpolar residue is not specified, and is varied combinatorially.^{10,11} The 3-dimensional structure of S-824 was determined recently by NMR, and as specified by the binary code design, it is a 4-helix bundle with a polar exterior and a hydrophobic core¹⁰ (Figure 1).

Protein S-824-C was nanografted onto a gold surface that had been previously covered with a monolayer of octadecanethiol (C₁₈). The nanografting procedure replaced the sulfur–gold interaction of the alkanethiol with a sulfur–gold interaction involving the C-terminal cysteine of the protein, as shown in Figure 2.

Experimental Procedures

(a) Mutagenesis, Protein Expression, Purification, and Characterization. DNA encoding protein S-824 was modified using PCR to add a glycine-glycine-cysteine linker at the C-terminal end of the protein sequence. This modified cysteine-containing sequence is called S-824-C. S-824-C was cloned into plasmid pET11a (Novagen). Protein was expressed in *E. coli* strain BL21 (DE3) grown in 2xYT. Protein was extracted from the cells using the freeze–thaw method¹² and then solubilized in 100 mM MgCl₂ containing 1 mM DTT (1,4-dithiothreitol). Cellular contaminants were removed by acid precipitation in 50 mM sodium acetate buffer (pH 4.2). The resulting supernatant was loaded onto a Poros HS cation exchange column (PerSeptive Biosystems) and eluted using a gradient of NaCl from 0 to 1.5 M. Purified protein was concentrated and exchanged into an AFM buffer using Centricon Plus-20 filters (Millipore).

The monomeric state of protein S-824-C in solution was confirmed using size exclusion chromatography (Superdex 75 HR/10/30 – Pharmacia) in 50 mM sodium phosphate buffer pH 7.4, 100 mM NaCl. In the presence of 1 mM TCEP (tris(2-carboxyethyl)phosphine) and 1 mM DTT, the cysteine was maintained in the reduced state and the protein was predominantly monomeric.

The concentration of protein in solution was measured by UV spectroscopy at 280 nm using a Hewlett-Packard 8452A diode

(8) (a) Yan, L.; Zhao, X. M.; Whitesides, G. M. *J. Am. Chem. Soc.* **1998**, *120*, 6179–6180. (b) Xia, Y.; Whitesides, G. M. *Angew. Chem., Int. Ed. Engl.* **1998**, *37*, 550–575.

(9) Kitagawa, K.; Morita, T.; Kimura, S. *J. Phys. Chem. B* **2004**, *108*, 15090–15095.

(10) Wei, Y.; Kim, S.; Fela, D.; Baum, J.; Hecht, M. H. *Proc. Natl. Acad. Sci. U.S.A.* **2003**, *100*, 13270–13273.

(11) (a) Wei, Y.; Liu, T.; Sazinsky, S. L.; Moffet, D. A.; Pelzer, I.; Hecht, M. H. *Protein Sci.* **2003**, *12*, 92–102. (b) Kamtekar, S.; Schiffer, J. M.; Xiong H.; Babik J. M.; Hecht M. H. *Science* **1993**, *262*, 1680–1685. (c) West, M. W.; Wang, W.; Patterson, J.; Mancias, J. D.; Beasley, J. R.; Hecht, M. H. *Proc. Natl. Acad. Sci. U.S.A.* **1999**, *96*, 11211–11216. (d) Hecht, M. H.; Das, A.; Go, A.; Bradley, L. H.; Wei, Y. *Protein Sci.* **2004**, *13*, 1711–1723.

(12) Johnson, B. H.; Hecht, M. H. *Biotechnology* **1994**, *12*, 1357–1360.

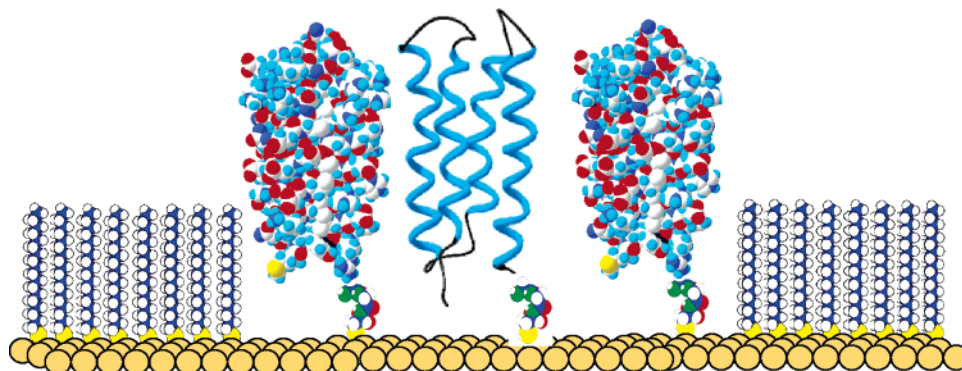


Figure 2. Schematic illustration of the 4-helix bundle protein S-824-C, with the Gly-Gly-Cys C-terminal linker nanografted into a C_{18} thiol layer on a gold surface. One of the protein molecules is shown as a ribbon diagram. The other two are shown in space filling representation of the known NMR structure. For clarity, the C_{18} monolayer is shown without the known 30° tilt.

array spectrophotometer. The extinction coefficient¹³ at 280 nm for protein S-824-C under the AFM buffer conditions is $6990 \text{ M}^{-1} \text{ cm}^{-1}$. Free sulfhydryl groups were assayed using Ellman's reagent.¹⁴

For AFM studies the protein was dissolved at $\sim 700 \mu\text{M}$ in a buffer containing 50 mM sodium acetate, pH 4.2, trifluoroethanol (10% v/v), and 1 mM TCEP. TCEP serves to keep the sulfhydryl groups reduced. Unlike DTT or mercaptoethanol, TCEP is not involved in the exchange reactions with self-assembled monolayers (SAMs) of thiols. During nanografting, the alkanethiols are displaced by thiol-terminated proteins. To enhance the solubility of the displaced alkanethiols 10% v/v trifluoroethanol (TFE) was added to the aqueous buffer.

It is known that cysteine headgroups form different SAMs than alkane thiols, because the main molecular axis is parallel to the gold surfaces.¹⁵ However, we do not expect this factor to have a major impact on our experiments because the glycine-glycine-cysteine linker at the C-terminus of the protein sequence should be flexible enough to allow the protein to orient into the most stable structure.

Circular dichroism (CD) spectroscopy measurements were performed using an Aviv model 62 DS spectropolarimeter, with protein dissolved in a buffer containing 50 mM sodium phosphate buffer (pH 7.4). Thermal unfolding experiments, monitored by CD, showed that the cysteine-terminated protein S-824-C had a similar stability to the parent S-824 protein. Although TFE is known to increase the α -helicity of unfolded polypeptides,¹⁶ CD spectroscopy showed that addition of TFE did not significantly change the α -helicity of the well-folded structure of protein S-824-C.

(b) Preparation of Alkanethiol SAMs. Gold surfaces were prepared by thermal deposition of gold onto mica surfaces. Mica substrates (Ruby Muscovite mica, S&J trading) were freshly cleaved before being placed into a high vacuum evaporator (K. J. Lekser Co. 1800 Bell Jar system). The evaporator was operated at 1×10^{-7} Torr before deposition and 1×10^{-6} Torr during deposition. The mica substrates were then heated for >8 h at 290°C before 1200 \AA gold (99.999% pure CERAC) films were deposited. This deposition process yields a surface composed of islands of single crystals of gold. The tops of these gold islands are plateaus, as large as 300 nm in lateral dimensions with few single atomic steps. After cooling in the evaporator, the gold substrates were taken out of the vacuum and immediately put into a 30 μM solution of $\text{SH}-(\text{CH}_2)_{17}-\text{CH}_3$ thiols (C_{18}) in 2-butanol and incubated for at least 48 h.

(c) AFM Imaging and Nanografting. Imaging was carried out using a Digital Instruments (Santa Barbara, CA) multimode Nanoscope III. Cantilevers were silicon nitride or oxide-sharpened (Digital Instruments) with a spring constant of 0.58 N m^{-1} . The scanner (Type E, Digital Instruments) had an accessible area of

$16.7 \times 16.7 \text{ mm}$ and was calibrated by measuring atomically resolved gold steps. All experiments were carried out in a liquid cell at room temperature.

Nanografting was accomplished via a three-step procedure: First the alkanethiol SAM was imaged by scanning at low force. These scans were done on the top of a gold single crystal island, where the surface is generally flat and only a few gold steps are visible. Second, an area of approximately $150 \text{ nm} \times 150 \text{ nm}$ was scanned at a force just above the threshold force to effectively remove the original C_{18} molecules. During this step, the proteins from the solution above the surface attach onto the freshly exposed gold surface and assemble to form a protein "island". Third, the freshly patterned surface was examined again at minimum forces.

Results

(a) Nanografting the Proteins into C_{18} Layers. In the five experiments in which we successfully nanografted protein S-824-C into C_{18} SAMs, we observed the formation of 15 patterns. A typical pattern is shown in Figure 3.

We measured the height of seven patterns. These heights were measured 400 times at variable forces (0–5 nN). Figure 4 shows a histogram of all height differences measured between the protein layers and the surrounding C_{18} matrix. Although there is a fairly large spread in the measurements, most of the measured heights fall in the range of 3–6 nm above the C_{18} matrix. Since the height of the C_{18} matrix is 2.2 nm above the gold surface, the measured heights indicate that the top of the protein is approximately 5–8 nm above the gold surface. To compare this with the expected height, we consider the heights of both the protein and the C-terminal Gly-Gly-Cys linker. The NMR structure of protein S-824 (without the linker) indicates the height of the 4-helix bundle is 4.5 nm. The height of the Gly-Gly-Cys linker in the fully extended form would be 1.3 nm. If not fully extended, its height would be approximately 1 nm. Thus, the height of the protein would be expected to be 5.5–5.8 nm above the gold surface. The discrepancy between the expected and observed heights is discussed below.

(b) Effect of Imaging Force on Patch Height. The viscoelastic properties of the nanografted protein patches were assessed by probing their response to an applied force. The height differences between the nanografted protein patches and the C_{18} matrix are plotted against the applied forces in Figure 5. In panel a, series 1–3 show sequential measurements of a single patch (the patch shown in Figure 3). In series 1 and 2, the force was increased from its minimum to 5 nN and all measurements were obtained sequentially in the time space of 30 min. In series 3, however, the same patch was scanned 3 h later with the force increased from its minimum to 6 nN. Comparison of series 1 with series 3 shows that, given

(13) Pace, C. N.; Vajdos, F.; Fee, L.; Grimsley, G.; Gray, T. *Protein Sci.* **1995**, *4*, 2411–2423.

(14) Ellman, G. L. *Arch. Biochem. Biophys.* **1959**, *82*, 70–77.

(15) Zhang, J.; Chi, Q.; Nielsen, J. U.; Friis, E. P.; Anderson, J. E. T.; Ulstrup, J. *Langmuir* **2000**, *16*, 7229–7237.

(16) (a) Buck, M. Q. *Rev. Biophys.* **1998**, *31*, 297–355. (b) Luo, Y.; Baldwin, R. L. *J. Mol. Biol.* **1998**, *279*, 49–57.

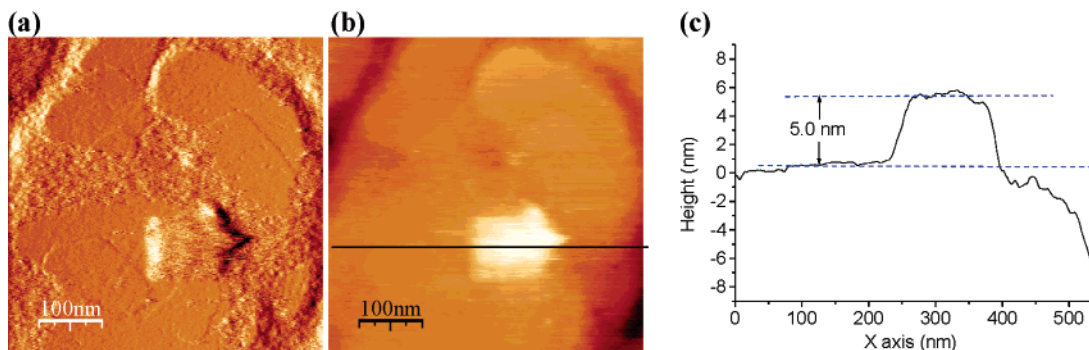


Figure 3. Panels a and b show the lateral deflection and height respectively of a 100 nm \times 100 nm protein patch nanografted into a C₁₈ layer on a gold island. There are a couple of gold steps in the 500 nm \times 500 nm area, which suggests that the surface is relatively flat. The nanografted protein patch is clearly visible as a bright area in panel b. (c) The height plot corresponds to the black line in the image in panel b. The height difference measured in this case is about 5.0 nm which corresponds to a total height of the patch of \sim 7 nm.

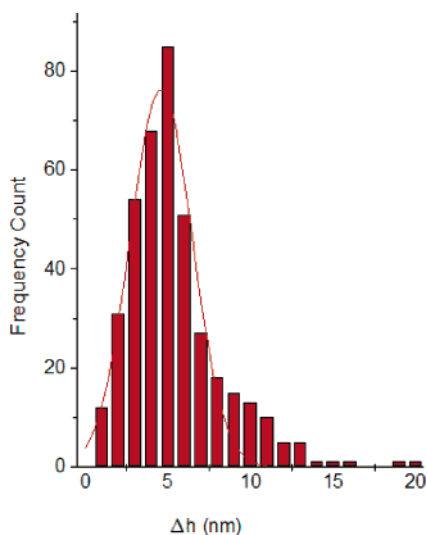


Figure 4. Histogram of the height differences (Δh) between grafted protein patterns and the C₁₈ matrix.

enough time, the patch recovers to its original state. Thus, these data show that the compression is reversible, and the protein patches are elastic. Panels b and c show similar measurements for two different patches.

The data shown in Figure 5 can be used to estimate the energy required to deform the immobilized protein molecules. The energy transferred from the tip to the sample is the integral of the product of the applied force times the resulting displacement, which is the area under the displacement vs force curve. This energy is approximately 30×10^{-18} J. The estimated size of the area of contact between the tip and the proteins is 1000 sq nm. According to the NMR structure of protein S-824, the cross-section of the protein at its widest point is approximately 3 nm \times 3 nm. Thus, the tip compresses (within a factor of 2) 100 protein molecules. Consequently, the energy required to deform a single protein molecule is approximately 30×10^{-20} J. This corresponds to 180 kJ/mol or 43 kcal/mol.

Figure 5a shows that the first two scans, obtained within the first 30 min, do not superimpose, whereas scan number 3 does agree with the first. This hysteresis demonstrates that recovery of the original structure is not instantaneous and indicates that energy is temporarily stored in the protein patch. This stored energy that corresponds to the area shaded gray between the two curves in panel 5a is approximately 12×10^{-18} J. Assuming 100 protein molecules are impacted by the tip (see above), this corresponds to 72 kJ/mol or 16.8 kcal/mol.

The data shown in panels b and c also show some hysteresis. Although further experiments will be required to determine the precise value of the energy stored per molecule, this value can be estimated from the experiments shown in Figure 5. Taking all of the data together, we estimate that the stored energy per molecule is 14 kcal/mol with an error of about 20%. (This error takes into account the dispersion of the data, but not the error in the estimate of the number of molecules that experience the force of the AFM tip, which as indicated above, is about a factor of 2.) We can compare this value to the ΔG of 7.7 kcal/mol measured for the unfolding of protein S-824 in solution.^{11a} Given (i) the uncertainties associated with the structure and packing density of protein S-824-C in the nanografted patches (see also the discussion section below), (ii) the dramatically different environments of the protein in the nanografted patches versus free in solution, and (iii) the substantial differences between a denatured monomeric protein in solution and a deformed protein compressed in a dense patch on a surface, these values are remarkably similar.

Finally, although it is clear that many more measurements must be done before this technique is fully validated, we feel that the present results are reproducible enough and tantalizing enough to suggest this method as a reliable way to determine the stability of a folded biopolymer in a monolayer.

(c) Threshold Force Required to Produce Protein Patterns. For nanografting, it is important to establish the threshold force required to remove the original thiol molecules without disturbing the underlying layer of gold. The threshold force is tested each time by gradually increasing the grafting force until a complete square pattern is made. For example, Figure 6 shows a pattern made by nanografting, with the tip scanning from top to bottom. Although the photodiode readings of the AFM cantilever were maintained constant, the intrinsic properties of the piezoelectric materials of the scanner cause the actual force between the tip and the sample to decrease slightly from the top to the bottom of the pattern. At the top, the force is just sufficient to remove the original thiol molecules, and a stable protein pattern is formed. However, at the bottom of the image, the force is not sufficient to remove the original thiol molecules; consequently, the C₁₈ layer remains mostly intact, and no protein layer is formed. This experiment demonstrates that penetration of the alkanethiols is a prerequisite for patch formation, thereby showing that the observed protein patches comprise proteins that are chemically adsorbed onto the freshly exposed gold and are not merely physically absorbed onto the C₁₈ SAMs.

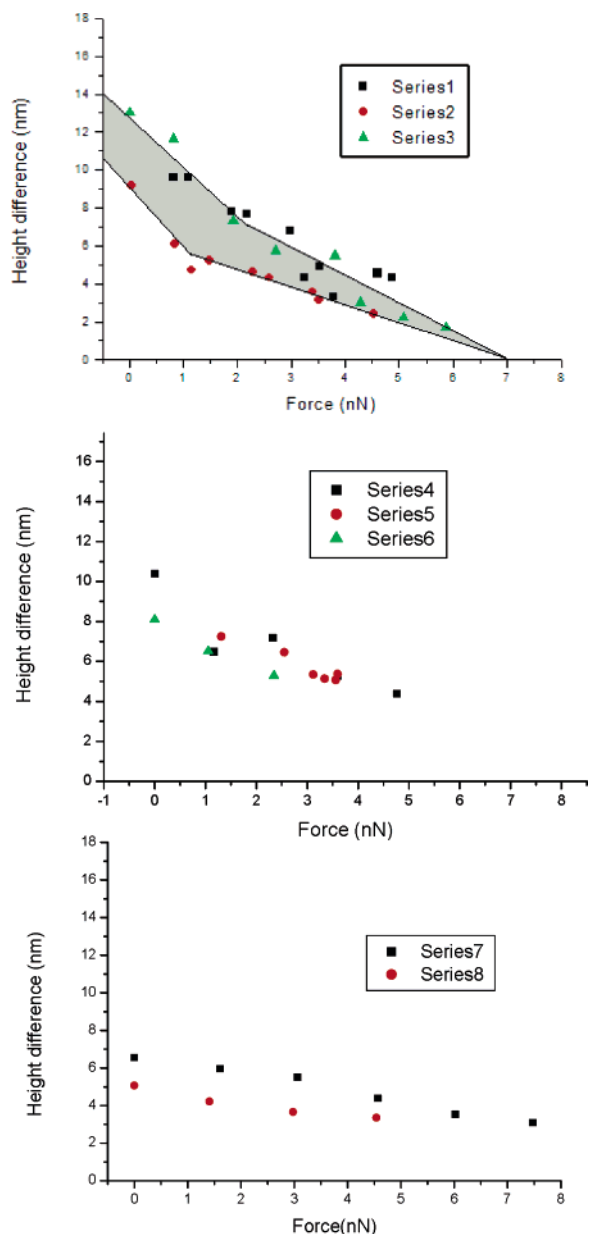


Figure 5. Height differences between grafted protein patches and the C_{18} matrix were measured as a function of the imaging force. (a) Series 1–3 are sequential studies of the same pattern. All scans were obtained starting at low force values and gradually increasing the force to its maximum values. Series 1 and 2 were obtained within the time span of 30 min, whereas series 3 was obtained 3 h later (a single scan lasts 1.5 min). The shaded area between the two curves represents the energy stored in the proteins compressed by the tip. (b) Series 4 through 6 show three series of height vs force scans of another protein patch. The series were obtained by starting at low force values and gradually increasing the force to its maximum values. All three scans were obtained in the time span of 25 min. (c) Series 7 and 8 show similar measurement done on another protein patch. Both series were obtained in a time span of 16 min.

(d) Self-Reorganized Protein Layers. Figure 7 shows a series of sequential images of a protein pattern. Initially, the patch was imaged at a low force after the proteins were nanografted (Figure 7a). The height of the patch is 5 nm higher than the surrounding C_{18} matrix. After this image was recorded, the pattern was scanned at high forces more than 40 times and then re-imaged at a low force. The resulting image is shown in Figure 7b. In this image (and other similar images), it is clear that the protein patch has been displaced. Next, the surface

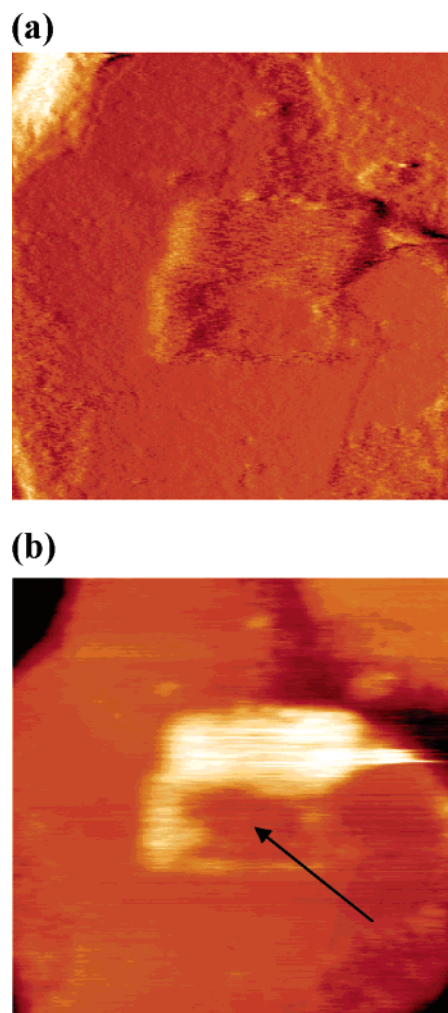


Figure 6. Panels a and b show the deflection and height, respectively, of a nanografted protein pattern. Even though the entire area ($\sim 200 \text{ nm} \times \sim 200 \text{ nm}$) in the center of the image was scanned, removal of the C_{18} layer and formation of a well-organized protein pattern was successful only at the top of the pattern (brightly colored area near center of panel b). The arrow points to the bottom of the pattern where the imaging forces are slightly lower than at the top. Note that around the arrow the C_{18} layer remained intact and only small amounts of protein were bound to the surface.

was soaked in a solution of protein for more than 24 h. The resulting surface was then re-imaged at a low force. This final image, shown in Figure 7c, reveals a new protein patch. This new patch again measures 5 nm higher than the surrounding C_{18} matrix. This study shows that during the 24-hour soaking, protein molecules can reabsorb onto a previously nanografted surface and self-assemble into an ordered layer.

This newly assembled (“self-reorganized”) patch is fragile and is damaged after just a few scans. Thus, the patterns made by the nanografting procedure are more stable and more robust than the self-organized protein patches. This is consistent with previous studies showing that nanografting of alkanethiol produce better packed layers than the surrounding self-organized monolayers of alkanethiols.⁷

(e) Patches Formed by Exchange of Proteins with Thiol Molecules in Defective Areas of the SAM. Defects in the C_{18} SAM can expose the underlying gold surface. The number and distribution of these defects depend on the compactness and order of the C_{18} layer.

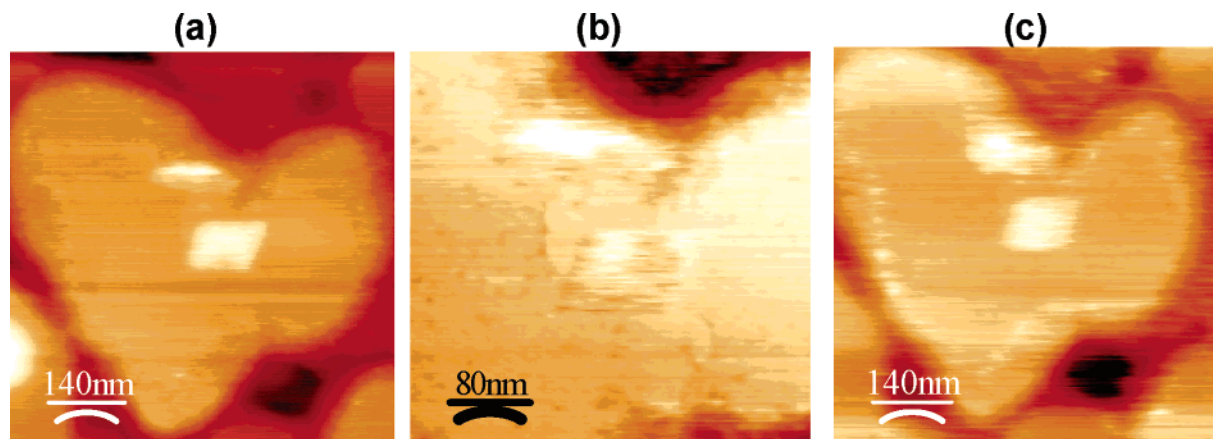


Figure 7. (a) Height image of the protein patch immediately after it was nanografted (white diamond shape in center of image). (b) Height image of the protein patches shows extensive damage after the surface was scanned many times at high force. This image is specifically zoomed in from $700 \text{ nm} \times 700 \text{ nm}$ to $400 \text{ nm} \times 400 \text{ nm}$ to show the details of the damage. (c) After the sample was soaked in protein solution for more than 24 h, a new protein patch self-assembled.

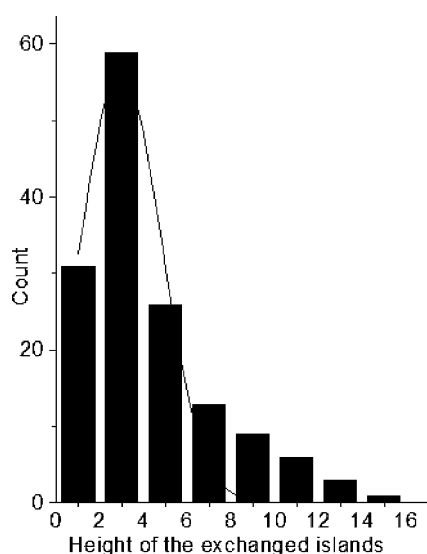


Figure 8. Histogram showing the distribution of heights above the C_{18} matrix for spontaneously exchanged islands. Each count represents the average of multiple measurements obtained from one image. An average of four to five readings was made for each of the 150 images. Overall, there are 1200 height measurements.

Because the C_{18} alkanethiol molecules surrounding these defects experience fewer van der Waals interactions with neighboring C_{18} alkanethiol molecules, they have an enhanced propensity to desorb from the gold surface. The resulting exposure of the gold surface provides a target for the spontaneous adsorption of protein molecules from the solution. These spontaneously exchanged islands can be as large as tens of nanometers.

We have observed many of these spontaneously exchanged islands. Figure 8 shows a histogram displaying the distribution of heights for 1200 measurements of 150 images of spontaneously exchanged islands. The maximum in the height distribution of the exchanged islands is 3 nm higher than the C_{18} matrix. This means that these exchanged patches of protein are approximately 5 nm high, which is close to the expected height of ~ 5.5 nm for the protein attached to the surface through a Gly-Gly-Cys linker.

Discussion

The studies reported herein demonstrate that a de novo 4-helix bundle isolated from a combinatorial library of

novel proteins can be nanografted into addressable patches on a gold surface. The approach described here for nanografting protein S-824-C is generally applicable to other proteins, whether natural or designed de novo. The generality of the approach is illustrated by the following: (i) Protein S-824-C was expressed from a synthetic gene cloned in *E. coli* and was purified using standard procedures applicable to most proteins, either natural or designed. (ii) The C-terminal Gly-Gly-Cys that provided an accessible thiol for nanografting was engineered into the protein by PCR-based mutagenesis procedures that can be applied to virtually any protein. (iii) The structure of protein S-824 is a 4-helix bundle, which is a common motif both in natural proteins and in proteins designed de novo.¹⁷ (iv) Finally, protein S-824, like many natural 4-helix bundles binds heme, a redox-active cofactor, which can enable electrochemical detection of ligand binding.¹⁸

Although we readily nanografted numerous patches of protein S-824-C, the experiments were technically challenging, and the nanografting protocol produced well-defined patches only in approximately one of three attempts. Even when protein patches were achieved, their measured heights varied and were not always identical to the expected height (see Figure 4). Moreover, the patches were relatively soft and compressible (see Figure 5).

The current study can be contrasted with our earlier study, wherein we nanografted a synthetic three α -helix metalloprotein $[\text{Fe}(\text{apVaLdC26})_3]^{2+}$ into a C_{18} SAM surface.¹⁹ In that study, we found that protein patches could be produced in nearly all attempts, the heights spanned a narrow range that was close to the expected height, and the heights remained constant at forces up to 25 nN.

Why does protein S-824-C produce patches less reliably and with lower stability than $[\text{Fe}(\text{apVaLdC26})_3]^{2+}$? To address this question, we note that S-824-C was bonded to the gold surface via a single cysteine thiol at the terminus of its 102 residue sequence, whereas $[\text{Fe}(\text{apVaLdC26})_3]^{2+}$ was bonded to the surface by three thiols, one at the end of each of its three 26-residue helices. The

(17) (a) Kamtekar, S.; Hecht, M. H. *FASEB J.* **1995**, *9*, 1013–1022. (18) (a) Moffet, D. A.; Certain, L. K.; Smith, A. J.; Kessel, A. J.; Beckwith, K. A.; Hecht, M. H. *J. Am. Chem. Soc.* **2000**, *122*, 7612–7613. (b) Moffet, D. A.; Case M. A.; House J. C.; Vogel, K.; Williams, R. D.; Spiro, T. G.; McLendon, G. L.; Hecht, M. H. *J. Am. Chem. Soc.* **2001**, *123*, 2109–2115. (c) Moffet, D. A.; Foley, J.; Hecht, M. H. *Biophys. Chem.* **2003**, *105*, 231–239. (d) Das, A.; Trammell, S. A.; Hecht, M. H. 2005 submitted. (19) Case, M. A.; McLendon, G. L.; Hu, Y.; Vanderlick, T. K.; Scoles, G. *Nano Lett.* **2003**, *3*, 425–429.

presence of a thiol anchor at the terminus of each helix apparently stabilized the protein–gold interaction and favored well-ordered protein patches.

For protein S-824-C, it was more difficult to produce well-defined patterns of uniform height. Moreover, as described above, there was a discrepancy between expected heights of the patches (based on the NMR structure of protein S-824) and the observed heights: The measured heights placed the top of the protein approximately 5–8 nm above the gold surface, whereas the expected height would have been 5.5–5.8 nm above the gold surface. Thus, the average heights observed in the experiments were higher than expected.

The taller-than-expected structures might be explained as follows: The entire protein (MW > 12 000) was bound to the gold surface by a single sulfhydryl on the Gly-Gly-Cys linker at the C-terminus of the protein. This tripeptide linker has a much smaller cross-section than the 4-helix bundle protein (see Figure 2). Therefore, if all of the sulfhydryl groups in a sample of protein seek the gold surface, then there would not be sufficient space for the 4-helix bundle proteins to pack. This situation is analogous to packing mushrooms:²⁰ If the vertical stems achieve close packing at their bases, then close packing will not be possible for the mushroom caps. This effect may destabilize the formation of 4-helix bundles in the nanografted patches and favor an alternative structure in which the protein refolds upon adsorption to the gold substrate. Such refolding might cause the α -helices to propagate through the first and third turns, thereby producing a long 2-helix hairpin rather than the shorter 4-helix bundle seen in solution and shown in Figure 1. The estimated height of this hairpin topology would be ~ 7.5 nm, rather than the 4.5 nm observed in the NMR structure of S-824 free in solution. The hydrophobic surface of such a hairpin would be buried partially in the hairpin itself and partially by dimerization with another hairpin. The resulting dimerized hairpin, a double-length 4-helix bundle, would minimize the “mushroom” phenomenon by maximizing the density of sulfhydryl residues at the gold and would account for the observation of patches that are higher than expected. Moreover, the occurrence of a mixed population, in which some proteins formed double-length hairpin structures while others retained the 4-helix bundle structure shown in Figure 1, might explain the relatively large range of heights observed in Figure 4.

(20) Wu, T.; Efimenko, K.; Genzer, J. *J. Am. Chem. Soc.* **2002**, *124*, 9394–9395.

In contrast to the nanografted patches, the self-exchanged patches exhibit a measured height above the gold substrate of approximately 5 nm, which is close to the height expected for the 4-helix bundle (Figure 1) attached to the surface through the Gly-Gly-Cys linker. Self-exchanged patches do not experience the confinement associated with nanografting and, therefore, would not feel the same lateral pressure to confine their widths by refolding into helical hairpins.

As discussed above, in our earlier studies with the synthetic 3-helix bundle [Fe(apVaLdC26)₃]²⁺, all three helices were terminated with cysteines. Consequently, that construct may have been easier to nanograft because it did not suffer the size incompatibility between the protein and the sulfhydryl linker. (That situation would be analogous to packing mushrooms, with each mushroom having 3 stems.)

Although further measurements are certainly needed to improve the precision of these studies, it is already clear that measuring the energy stored in proteins by mechanical compression shows considerable promise as a method for probing the structural stability of proteins packed at high density. This approach will be particularly powerful if time-resolved measurements are used to reveal the relative relaxation times.

In summary, our results demonstrate that de novo proteins can readily be nanografted onto gold surfaces. Moreover, both synthetic 3-helix metalloproteins and genetically expressed binary patterned 4-helix bundles from combinatorial libraries can serve as nanografting samples. The variety of results observed for these two systems indicate that, prior to the incorporation of nanografted proteins into nanoscale biosensors, further studies must be conducted to optimize the protein-surface interactions.

Acknowledgment. This work was supported by the Department of Energy Grant 340-6007 (G.S.) and by NIH Grant R01 GM062869 (M.H.H.). The authors are very grateful to an anonymous referee for an extremely thoughtful analysis of our work and for recommending important improvements, including the suggestion that S-824-C might form helical hairpins in nanografted patches and, most importantly, that the data of Figure 5 might allow an estimate of the energy stored in the proteins.

LA046857H